Theoretical Modeling and Optimization of Porous Coating for Hypersonic-laminar-flow Control

Journal:	*AIAA Journal*
Manuscript ID	2018-03-J057272.R1
Manuscript Type:	Express Article
Date Submitted by the Author:	09-May-2018
Complete List of Authors:	Zhao, R.; Beijing Institute of Technology; Hong Kong Polytechnic University, Mechanical Engineering Liu, Tuo; Hong Kong Polytechnic University, Mechanical Engineering Wen, Chihyung; The Hong Kong Polytechnic University, Department of Mechanical Engineering Zhu, Jie; The Hong Kong Polytechnic University, Department of Mechanical Engineering Cheng, L.; Hong Kong Polytechnic University, Mechanical Engineering
Subject Index Category:	20400 Boundary-Layer Stability and Transition < 20000 FLUID DYNAMICS, 20700 Hypersonic Flow < 20000 FLUID DYNAMICS, 20500 Computational Fluid Dynamics < 20000 FLUID DYNAMICS
Select ONE Subject Index for the Table of Contents. This is where your paper will show up in the Table of Contents:	20000 FLUID DYNAMICS

Theoretical Modeling and Optimization of Porous Coating for Hypersonic-laminar-flow Control

R. Zhao *
Beijing Institute of Technology, Beijing, 100081, China
The Hong Kong Polytechnic University, Kowloon, Hong Kong Special Administrative Region

and

T. Liu, † C. Y. Wen, ‡ J. Zhu, § and L. Cheng **
The Hong Kong Polytechnic University, Kowloon, Hong Kong Special Administrative Region

We develop a theoretical model to describe the acoustic characteristics of plane ultrasonic acoustic waves imping on a porous coating, a rigid surface periodically corrugated with subwavelength grooves (two-dimensional cavities). The proposed model takes into account the high-order diffracted modes and therefore incorporates mutual coupling among neighboring cavities. The model predicts a reflection frequency consistent with the numerical results and reproduces a coupling mode induced by interactions between waves scattered from adjacent cavities. With this model, the cavity geometry parameters are optimized to achieve the minimum reflection coefficient. The result shows that the Mack second mode is strongly suppressed and that the maximum fluctuating pressure decreases by about 88% upon using the optimized porous coating in a Mach 6 flat-plate flow.

Nomenclature

(Nomenclature entries should have the units identified)

A = porous layer admittance

A_r = cavity aspect ratio, $2b/H$

b = cavity half-width

H = thickness of porous layer

f_{acs} = normalized acoustic frequency, $f H/a_w$

* Assistant Professor, School of Aerospace Engineering; Research Assistant, Department of Mechanical Engineering
† Ph.D. Candidate, Department of Mechanical Engineering
‡ Professor, Department of Mechanical Engineering, Associate Fellow AIAA
§ Assistant Professor, Department of Mechanical Engineering
** Professor, Department of Mechanical Engineering

R = reflection coefficient

T = temperature

t = time

x, y = streamwise and normal directions

ω = angular frequency

ϕ = porosity, $2b/s$

ρ = density

Subscripts

i = incident waves

r = diffracted waves

c = waves in the cavity

w = parameters at the wall

∞ = free stream

I. Introduction

VARIOUS techniques have been developed to prevent or delay the hypersonic boundary-layer transition [1–3]. One of the most promising control technologies is the passive porous coating concept proposed by Fedorov *et al*.[4] because of its minimal effect on mean flow and the effective suppression of the most unstable boundary-layer instability; namely, the Mack second mode [5–7]. The effect of a porous coating on the hypersonic boundary layer could be either theoretically interpreted by the porous boundary condition of vertical velocity at the wall: $v'_w=Ap'_w$ [4, 8], or numerically investigated by directly resolving the flowfield within the microstructures [9-11]. The first method is more convenient when we focus on the influences of the geometry parameters of microstructures without the need to modify the computational mesh. The admittance A is a complex quantity that depends on the properties of the wall material, porosity parameters, mean flow characteristics at the wall surface, and flow-perturbation parameters such as wave frequency and wavelength. The equation for admittance is derived by applying the theory of sound wave propagation in a thin long tube [12]. Although this theoretical model, hereinafter called Fedorov's model, has been widely applied (see recent works in Refs. [13–15]), it does not take into account the high-order diffracted waves, and

thus underestimates the coupling among adjacent cavities as well as its contribution to the overall admittance [16–18]. This simplification is considered to be responsible for the low-frequency shift of the reflection curves [14,19]. The design of this porous coating device and its integration with thermal protection systems require the development of accurate models of the effect of the porous coating. In particular, further optimization requires frequency matching between the most amplified Mack second-mode instability wave and the minimum reflection property of microstructures.

In the present study, we improve the porous coating model by considering high-order diffracted waves when the acoustic disturbance penetrates the porous surface. In this way, the scattering and coupling effect is more carefully taken into account. Based on the proposed model, a straightforward optimization procedure is introduced to maximize the absorption of the porous layer.

II. Theoretical Model and Optimization

As shown in Fig. 1, the porous surface is a rigid surface periodically corrugated with subwavelength grooves (two-dimensional cavities) being infinitely extended in the x direction. The background medium is assumed to have uniform and constant density ρ_w and sound speed c_w. The subscript w denotes the local physical quantity at the wall. The half-width and depth of the cavities are b and H, respectively, with the unit-cell period being s. The porosity and aspect ratio are $\phi = 2b/s$ and $Ar = 2b/H$, respectively. These definitions are in accordance with previous research [14,19].

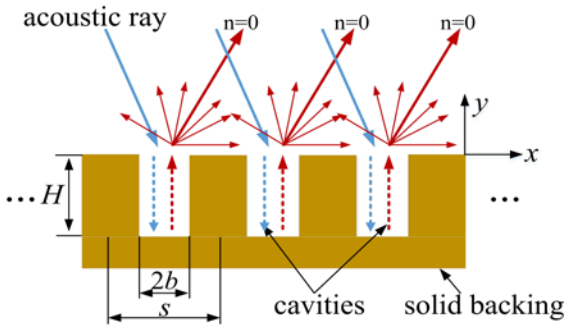

Fig. 1 Schematic drawing of reflection of acoustic waves from equally spaced two-dimensional cavities.

The acoustic field and the surface admittance of such textured surface can be analytically obtained on the plane wave expansion method [16-18]. An obliquely incident plane acoustic wave can be written as (the time dependence $e^{-j\omega t}$ is omitted for simplicity)

$$p_i = e^{jk_x x} e^{-jk_y y},$$
$$v_{y,i} = \frac{1}{j\omega\rho_w}\frac{\partial p_i}{\partial y} = -\frac{k_y}{\rho_w \omega} e^{jk_x x} e^{-jk_y y}, \tag{1}$$

where p_i is the incident pressure, $v_{y,i}$ is the y component of the particle velocity, and $j = \sqrt{-1}$. k_x is the parallel momentum and $k_y = (k_0^2 - k_x^2)^{1/2}$ is the perpendicular momentum, in which $k_0 = \omega/c_w$ is the wavenumber with ω being the angular frequency. The reflected pressure field p_r^n and y-component particle velocity $v_{y,r}^n$ of the nth-order diffracted wave are expressed as

$$p_r^{(n)} = R_n e^{jk_x^{(n)} x} e^{jk_y^{(n)} y},$$
$$v_{y,r}^{(n)} = \frac{k_y^{(n)}}{\rho_w \omega} R_n e^{jk_x^{(n)} x} e^{jk_y^{(n)} y}, \tag{2}$$

where $k_x^{(n)} = k_x + 2\pi n/s$, $k_y^{(n)} = [k_0^2 - (k_x^{(n)})^2]^{1/2}$, $n \in \mathbf{Z}$ and R_n is the reflection coefficient of the nth-order diffraction. Inside the cavities, the fundamental wave mode dominates for long wavelengths limit ($2b \ll \lambda_{acs}$, where λ_{acs} is the wavelength of the incident acoustic wave), and the sound pressure and particle velocity within the cavity are denoted as

$$p_c = C_1 e^{jk_c y} + C_2 e^{-jk_c y},$$
$$v_{y,c} = \frac{k_c}{\tilde{\rho}\omega}\left(C_1 e^{jk_c y} - C_2 e^{-jk_c y}\right), \tag{3}$$

where the dynamic density $\tilde{\rho}$, compressibility $\tilde{C}$, and wavenumber k_c are complex and frequency-dependent quantities owing to the thermal and viscous boundary layers inside the narrow cavity,

$$\tilde{\rho} = \rho_w / \Psi_v, \tilde{C} = \frac{\gamma - (\gamma - 1)\Psi_t}{\rho_w c_w^2},$$
$$k_c^2 = \omega^2 \tilde{\rho}\tilde{C} = k_0^2 \frac{\gamma - (\gamma - 1)\Psi_t}{\Psi_v}. \tag{4}$$

Here, $\Psi_i = 1 - \tan(k_i b)/k_i b$ with

$$k_i^2 = \begin{cases} k_v^2 = j\omega\dfrac{\rho_w}{\mu}, & \text{viscous wave number} \\ k_t^2 = j\omega\dfrac{\rho_w C_p}{\kappa}, & \text{thermal wave number.} \end{cases}$$

The subscript i is either v or t to denote the effects of viscous or thermal boundary layers, respectively. In the above equations, κ is thermal conductivity, μ is viscosity, $\gamma = C_p/C_v$ is the ratio of the specific heat at constant pressure, C_p, to specific heat at constant volume, C_v.

The bottom of the cavity is rigid ($v_{y,c}|_{y=-H} = 0$), thus $C_1 = C_2 e^{2jk_c H} \equiv Ce^{2jk_c H}$. At the interface between the upper half space and the cavity opening mouth, the sound pressure should be continuous:

$$\frac{1}{2b}\int_{x=-b}^{x=b}\left(e^{jk_x x} + \sum_{n=-\infty}^{+\infty} R_n e^{jk_x^{(n)} x}\right)dx = C\left(1+e^{2jk_c H}\right). \tag{5}$$

Equation (5) is then deduced as

$$\sum_{n=-\infty}^{+\infty}\left(\delta_{n,0} + R_n\right)S_n = C\left(1+e^{2jk_c H}\right), \tag{6}$$

where $S_n = (2b)^{-1}\int_{-b}^{b} e^{jk_x^{(n)} x}dx = \mathrm{sinc}(k_x^{(n)} b)$ is the overlap integral between the nth-order diffracted mode and the fundamental mode inside the cavity, and $\delta_{n,0}$ is the Kronecker delta function defined as $\delta_{n,0} = 1$ for $n = 0$ and $\delta_{n,0} = 0$ otherwise.

As for the requirement of continuous particle velocity v_y at the interface, one may further obtain

$$-\frac{k_y}{\rho_w \omega}e^{jk_x x} + \sum_{n=-\infty}^{+\infty}\frac{k_y^{(n)}}{\rho_w \omega}R_n e^{jk_x^{(n)} x} = \begin{cases}\dfrac{k_c}{\tilde{\rho}\omega}C\left(e^{2jk_c H}-1\right), & x \in (-b,b)\\ 0, & x \notin (-b,b).\end{cases} \tag{7}$$

Multiplying Eq. (7) by $e^{-jk_x^{(r)} x}$ ($r \in \mathbf{Z}$), and averaging over the unit-cell area, we have

$$R_r = \delta_{r,0} - C\left(1-e^{2jk_c H}\right)\phi\frac{\rho_w k_c}{\tilde{\rho}k_y^{(r)}}S_r\,. \tag{8}$$

Substituting Eq. (8) into the pressure continuity condition (6) yields

$$2S_0 - C\left(1-e^{2jk_c H}\right)\phi^2\frac{\rho_w}{\tilde{\rho}}\sum_{r=-\infty}^{+\infty}\frac{k_c}{k_y^{(r)}}S_r^2 = C\left(1+e^{2jk_c H}\right). \tag{9}$$

The coefficient C can be determined from Eq. (9) and is then substituted into Eq. (8). The reflection coefficients of Eq. (9) are determined to be

$$R_n = \delta_{n,0} + \frac{2j\tan(k_c H)\phi\dfrac{\rho_w}{\tilde{\rho}}S_n\dfrac{k_c}{k_y^{(n)}}}{1 - j\tan(k_c H)\phi\dfrac{\rho_w}{\tilde{\rho}}\displaystyle\sum_{r=-\infty}^{+\infty}\frac{k_c}{k_y^{(r)}}S_r^2}. \tag{10}$$

For second-mode instability waves, normal incidence may be hypothesized, i.e., k_x=0 and k_y=k_0 [19]. As a result, the formulations of v_i, p_i and $v_r^{(n)}$, $p_r^{(n)}$ are greatly simplified. Assuming that the periodicity $s \ll \lambda_{acs}$, the effective admittance A can be derived as

$$A = \frac{v}{p}\bigg|_{y=0} = \frac{s^{-1}\int_{-s/2}^{s/2}\left(v_i + \sum_{n=-\infty}^{+\infty} v_r^{(n)}\right)\Big|_{y=0} dx}{s^{-1}\int_{-s/2}^{s/2}\left(p_i + \sum_{n=-\infty}^{+\infty} p_r^{(n)}\right)\Big|_{y=0} dx} = \frac{\int_{-s/2}^{s/2}\left(-\frac{k_0}{\rho_w\omega} + \sum_{n=-\infty}^{+\infty}\frac{\sqrt{k_0^2-\left(\frac{2\pi n}{d}\right)^2}}{\rho_w\omega} R_n e^{j\frac{2\pi n}{s}x}\right)dx}{\int_{-s/2}^{s/2}\left(1+\sum_{n=-\infty}^{+\infty} R_n e^{j\frac{2\pi n}{s}x}\right)dx} \tag{11}$$

$$= \frac{\frac{k_0}{\rho_w\omega}\int_{-s/2}^{s/2}(R_0-1)dx}{\int_{-s/2}^{s/2}(R_0+1)dx} = \frac{1}{\rho_w c_w}\frac{R_0-1}{R_0+1},$$

where the reflection coefficient of the zero-order diffraction (specular refraction) is

$$R_0 = 1 + \frac{2j\tan(k_c H)\phi\frac{\rho_w}{\tilde{\rho}}\frac{k_c}{k_0}}{1 - j\tan(k_c H)\phi\frac{\rho_w}{\tilde{\rho}}\sum_{r=-\infty}^{+\infty}\frac{k_c}{\sqrt{k_0^2-\left(\frac{2\pi r}{s}\right)^2}}S_r^2}. \tag{12}$$

Note that all higher-order diffracted modes are evanescent and cannot radiate to far field for normal incidence at low frequencies ($s/\lambda_{acs} \le 1$).

Fedorov's model is first calculated for an isolated deep cavity and then multiplied by porosity ϕ to treat the structured surface as a homogenous surface of uniform effective acoustic admittance [4]. Therefore, the diffracted waves coming from the opening mouth are not considered. To evaluate the overall effect when a plane wave penetrates a porous surface, the present model considers an infinite array of grooves. Because higher-order diffracted modes are included in the derivation, the mutual coupling between disturbances from neighboring cavities is taken into account. In particular, if we neglect all higher-order modes and let the porosity ϕ approach 0 (the local oscillation inside each cavity is independent), Eq. (12) reduces to Fedorov's model [12,14],

$$A = \frac{\phi}{Z_c} j\tan(k_c H), \tag{13}$$

where $Z_c = \tilde{\rho}\omega / k_c$ is the characteristic impedance inside the cavity.

Fig. 2 shows the reflection coefficients of plane monochromatic ultrasonic waves penetrating a porous surface in a quiescent and uniform-temperature atmosphere, with the two above-mentioned theoretical models, numerical results of Brès *et al.* [14], and by a finite-element solver (COMSOL Multiphysics®). The porous parameters are taken from Brès *et al* [14], and listed as a combination of Ar = 0.12, 0.3 and ϕ = 0.2, 0.48, 0.8. It should be noted that some of the high-order diffracted modes become propagative and thus radiate into the propagating mode in free space, when $s/\lambda_{acs} > 1$ [16]. The specular reflection is obfuscated with high-order diffractions in the upper half-space and cannot be separated from the superposed sound field in our full-wave simulation by COMSOL. Therefore, we did not provide the data when $f_{acs} > 0.67$, i.e. $s/\lambda_{acs} > 1$ for the case in Fig. 2(a). Here, $f_{acs} = f\,H/c_w = H/\lambda_{acs}$ is the normalized incidence-wave frequency [14], and $H/s = \phi/Ar = 0.67$ for the case in Fig. 2(a). Also, we would like to emphasize that $s/\lambda_{acs} = 1$ is a reasonable upper limit of the theoretical model. Actually, the numerical results of Brès *et al.* [14] were also cut off before $f_{acs} = 0.67$ for the case in Fig. 2(a), but they declared the calculation was strongly affected by the presence of a resonant acoustic mode of frequency $f_{res} = \phi/Ar$ [20]. In addition, they only showed the results before $f_{res}/2$ for the case in Fig. 2(b), and attributed the reason to the first subharmonic mode [20]. Nevertheless, the influences of the first subharmonic mode are not observed in other cases. For all cases, the predictions of the proposed model basically coincide with the numerical results from COMSOL and Brès *et al.* [14], even at high frequency when the wavelength λ_{acs} decreases to the same order of magnitude as s and the interaction of the scattered waves at the porous surface becomes strong; for instance, at $f_{acs} = 0.67$ in Fig. 2(a), when the ratio s/λ_{acs} approaches unity. Comparatively, Fedorov's model tends to shift the predicted frequency because it neglects the higher-order diffracted modes. Despite the homogenous hypothesis of $s \ll \lambda_{acs}$ for both theoretical models, the present model shows the advantage of predicting results that are consistent with numerical results up to the limit $s/\lambda_{acs} = 1$. In particular, when $s/\lambda_{acs} = 1$, a coupling acoustic mode is reportedly induced by the interaction of waves scattered from adjacent cavities [14, 20] and greatly decreases the absorption of the porous coating. This coupling mode is well reproduced by the proposed model, with the predicted $|R|$ approaching unity. For further illustration, we calculate the distributions of $|R|$ as a function of porosity ϕ at constant Ar = 0.3. As shown in Fig. 3, the maximum $|R|$ appears along the diagonal (dashed line) of the contour plot, where the incident-wave frequency f_{acs} approaches ϕ/Ar. This observation is exactly the same expression of coupling frequency f_{res} advocated by Brès *et al*. based on direct numerical simulation [14,19,20]. Additionally, when the incident-wave frequency is much lower than f_{res}, both theoretical models above give results that are consistent with numerical results [Fig. 2 (d)]. Moreover, Fig. 3 shows that the minimum $|R|$ can be achieved by optimizing cavity-

shape parameters. Brès *et al*. [19] deduced an expression of optimum cavity depth to ensure the phase opposition between the reflection from the solid wall and from the porous surface. However, R is a nonlinear function of the porosity parameters and flow quantities [Eq. (13)]. A numerical solution seems to be an effective way to obtain the minimum $|R|$ by applying triple program loops in the following order: loop 1: $0.2 \le \phi \le 0.8$, loop 2: $0.06 \le Ar \le 0.3$, loop 3: $0 < f_{acs} < \min(\phi/Ar, 2.0)$. These parameters span the range of interest for practical applications [14] and also ensure the accuracy of the proposed model.

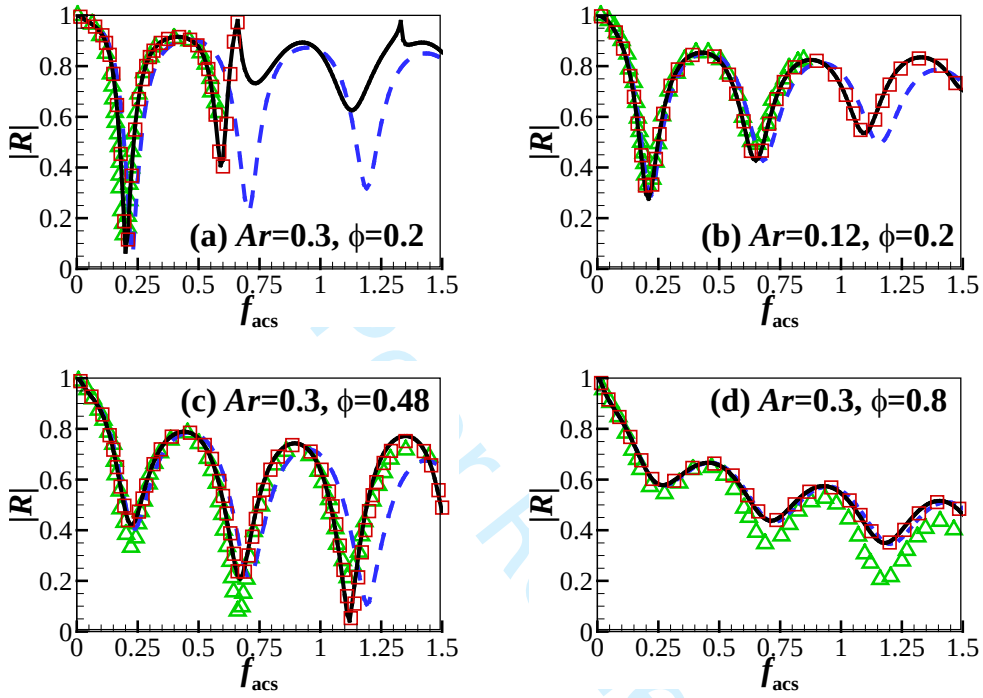

Fig. 2 Reflection coefficient amplitudes at normal incidence from numerical simulation by COMSOL (squares), numerical results of Brès et al. [14] (triangle), Fedorov's model (dashed line), and proposed model (solid line). $f_{acs}=f\,H/c_w$ is the normalized incidence-wave frequency.

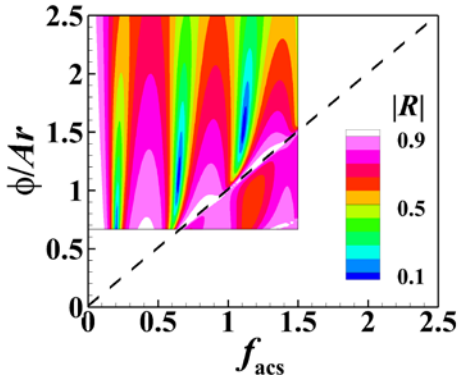

Fig. 3 Contours of reflection coefficient amplitude obtained from proposed theoretical model.

To confirm the proposed optimization strategy, we numerically study the stabilization problem of a hypersonic flow along a two-dimensional flat plate at zero angle of attack (Fig. 4). The freestream flow conditions are the same as in the experiment of Bountin *et al.* [21]: Mach number $Ma_\infty = 6.0$, unit Reynolds number $\mathrm{Re}_\infty = 10.5 \times 10^6\ \mathrm{m}^{-1}$, and temperature $T_\infty = 43.18$ K. The wall is isothermal with temperature $T_w = 293$ K. The numerical method and code validation is available in Ref. [22]. An unsteady disturbance is introduced at the beginning of the plate by a slot of periodic suction-blowing at the fixed frequency of 138.74 kHz. The porous coating covers the second half of the plate, and its effect is modeled by the boundary condition $v'_w = Ap'_w$ at the wall. Because the sound speed c_w is determined by T_w, the remaining input flow parameter for Eq. (13) is ρ_w. In this case, we use the value of ρ_w at $x/L_{ref} = 0.75$, and the optimized shape parameters are $\phi = 0.66$, $Ar = 0.28$, and $f_{acs} = 0.67$. With these shape parameters, the streamwise minimum $|R|$ is 3.4×10^{-5} at $x/L_{ref} = 0.75$, and the maximum $|R|$ is 2.9×10^{-3} at $x/L_{ref} = 0.5$. For comparison, the performance of a conventional porous coating [14] with relatively deep cavities ($\phi = 0.66$, $Ar = 0.1$, and $f_{acs} = 1.87$) is also presented.

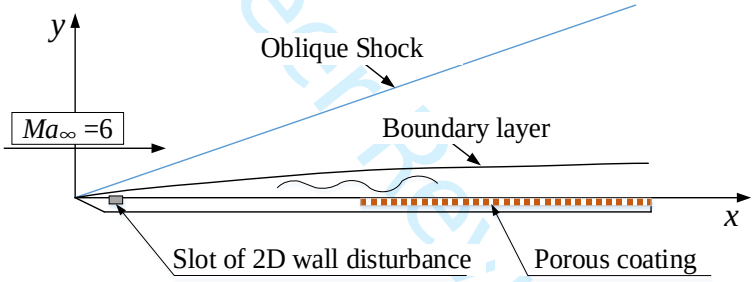

Fig. 4 Schematic drawing of problem formulation. Porous coating is at $0.5 \le x/L_{ref} \le 1.0$, $L_{ref} = 0.2$ m is the reference length.

Fig. 5 shows the instantaneous contours of fluctuating pressure, and Fig. 6 compares the amplitude distributions of fluctuating pressure for the three cases. According to Ref. [22], Mack second mode dominates along the second half of the plate. Taking the baseline case as an example [Fig. 5(a)], two-cell structures form downstream ($x/L_{ref} > 0.5$) with longitudinal wavelength approximately equal to twice the boundary-layer thickness, which corresponds to the typical Mack second-mode structure [23]. Upon installing the porous coating, the Mack second mode is strongly suppressed, especially for the optimized case [Fig. 5(b)]. Notably, upstream of the porous coating, the strong oscillations in Fig. 6 result from the coexistence of multiple waves (including mode *F* and mode *S* of acoustic waves, and entropy/vorticity waves) in the boundary layer [13, 22]. Compared with the baseline case and the conventional porous coating, the maximum fluctuating pressure for the optimized case decreases by 88% and 30%, respectively.

Also, the optimized shallow cavity is easier to manufacture. For the second-mode wave packets having a frequency band between 88.28kHz and 176.58kHz (referred to [21]), the calculated $|R|$ of the optimized porous coating varies more obviously than those of the conventional one, and its advantage can only be found in a narrow frequency band between 124.5kHz and 153.8kHz (Fig. 7). It suggests a porous coating consisting of varied-depth cavities, such as a gradient coating [18], will be a potential candidate to suppress the disturbance with broadband frequencies. Once again, the Fedorov's model shifted the predicted frequency at the optimized shape parameters since it neglects the higher-order diffracted modes (Fig. 7).

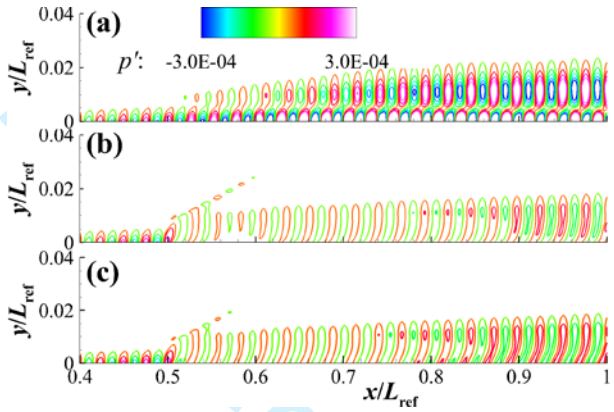

Fig. 5 Instantaneous fluctuating pressure fields (p' is normalized by $\rho_\infty u_\infty^2$, and ρ_∞ and u_∞ are the freestream density and velocity, respectively): (a) baseline case without porous coating; (b) optimized porous coating; (c) conventional porous coating with relatively deep cavities.

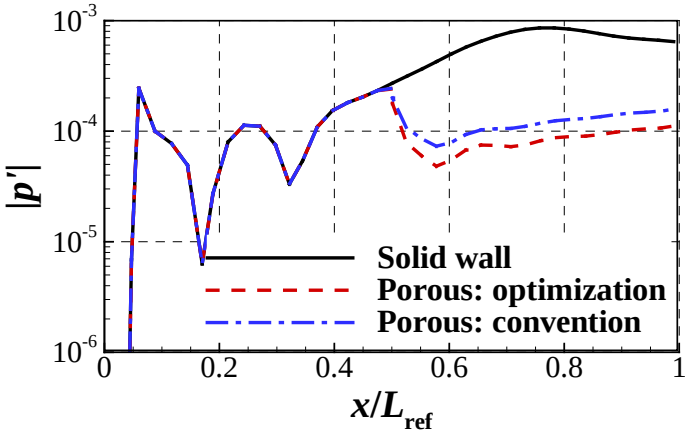

Fig. 6 Amplitude distributions of pressure perturbation along the wall (p' is normalized as the way in Fig. 5).

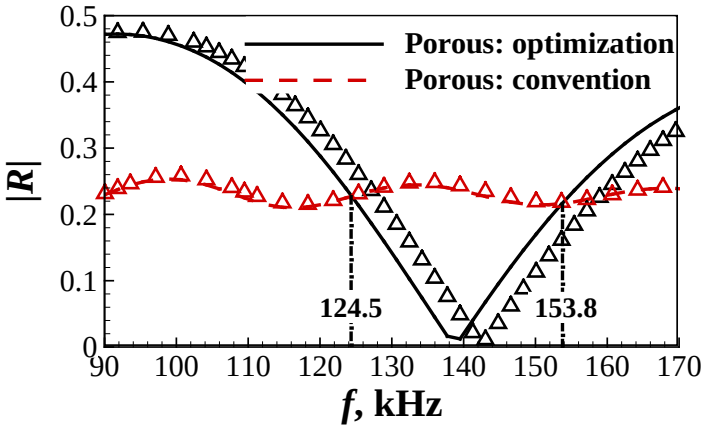

Fig. 7 Calculated reflection coefficients for different disturbance frequencies. Line: calculated by the proposed model, Symbol: calculated by Fedorov's model.

III. Conclusion

In conclusion, we propose herein an improved theoretical model describing how a porous coating affects the control of the hypersonic boundary-layer transition, taking into account the higher-order diffraction waves generated at the porous surface. Compared with the results of Fedorov's model, the reflection frequency predicted by the proposed model is consistent with numerical data and reproduces the coupling mode between adjacent cavities. Additionally, a straightforward optimization strategy involving program loops is introduced. The Mack second mode is strongly suppressed by the optimized porous coating, with the maximum fluctuating pressure decreasing by about 88%. For the second-mode wave packets having a frequency band, an optimized porous coating with varied-depth cavities will be explored in a future study. This work also indicates that similar theoretical models could be developed to describe porous coatings with pores or cavities of different cross sections.

Acknowledgments

This study was supported by the Research Grants Council, Hong Kong under Contract No. C5010-14E and the National Natural Science Foundation of China under Grant No. 11402024. We express our honest appreciation to Professor Li Xinliang for his generosity in providing the direct numerical simulation codes.

References

1. Krishnan, K. S. G., Bertram, O. and Seibel, O., "Review of hybrid laminar flow control systems," *Progress in Aerospace Science*. Vol. 93, 2017, pp. 24–52.

doi: 10.1016/j.paerosci.2017.05.005

2. Maslov, A. A., "High Speed Boundary Layer Stability and Control," *AIP Conference Proceedings*, Vol. 1376, 2011, pp. 18–22.

doi: 10.1063/1.3651827

3. Fedorov, A. V., "Prediction and Control of Laminar-turbulent Transition in High-speed Boundary-Layer Flows," *Procedia IUTAM*, Vol. 14, 2015, pp. 3–14.

doi: 10.1016/j.piutam.2015.03.

4. Federov, A. V., Malmuth, N. D., Rasheed, A., and Hornung, H. G., "Stabilization of Hypersonic Boundary Layers by Porous Coatings," *AIAA Journal*, Vol. 39, No.4, 2001, pp. 605–610.

doi: 10.2514/3.14776

5. Mack, L. M., "Boundary-layer Stability Theory", Jet Propulsion Laboratory, California Institute of Technology, Pasadena, California, November, 1969.

6. Chokani, N., "Nonlinear Evolution of Mack Modes in a Hypersonic Boundary Layer," *Physics of Fluids*, Vol. 17, No. 014102, 2005.

doi: 10.1063/1.1825471

7. Fedorov, A., "Transition and Stability of High-Speed Boundary Layers," *Annual Review of Fluid Mechanics*, Vol. 43, 2011, pp. 79–95.

doi: 10.1146/annurev-fluid-122109-160750

8. Fedorov, A. V., Shiplyuk, A. N., Maslov, A. A., Burov, E., and Malmuth, N. D., "Stabilization of a Hypersonic Boundary Layer using an Ultrasonically Absorptive Coating," *Journal of Fluid Mechanics*, Vol. 479, 2003, pp. 99–124.

doi: 10.1017/S0022112002003440

9. Sandham, N.D. and Lüdeke, H. "A Numerical Study of Mach 6 Boundary-Layer Stabilization by Means of a Porous Surface," *AIAA Journal*. Vol. 47, No. 9, 2009, pp. 2243-2252.

doi: 10.2514/1.43388

10. Wartemann, V., Lüdeke, H. and Sandham, N.D. "Numerical Investigation of Hypersonic Boundary-Layer Stabilization by Porous Surfaces," *AIAA Journal*, Vol. 50, No. 6, 2012, pp. 1281-1290.

doi: 10.2514/1.J051355

11. Kirilovskiy S. V., Poplavskaya T. V., Tsyryulnikov I. S., and Maslov A.A. "Evolution of Disturbances in the Shock Layer on a Flat Plate in the Flow of a Mixture of Vibrationally Excited Gases," *Thermophysics and Aeromechanics*, Vol. 24, No. 3, 2017, pp. 421–430.

doi: 10.1134/S0869864317030106

12. Kozlov, V. F., Fedorov, A. V, and Malmuth, N. D., "Acoustic Properties of Rarefied Gases inside Pores of Simple Geometries," *The Journal of the Acoustical Society of America*, Vol. 117, No. 6, 2005, pp. 3402–3412.
doi: 10.1121/1.1893428

13. Wang, X., and Zhong, X., "The Stabilization of a Hypersonic Boundary Layer using Local Sections of Porous Coating," *Physics of Fluids*, Vol. 24, No. 034105, 2012.
doi: 10.1063/1.3694808

14. Brès, G. A., Inkman, M., Colonius, T., and Fedorov, A. V, "Second-mode Attenuation and Cancellation by Porous Coatings in a High-speed Boundary Layer," *Journal of Fluid Mechanics*, Vol. 726, 2013, pp. 312–337.
doi: 10.1017/jfm.2013.206

15. Lv, P., Yu, C., Zhang, Y., and Gong, J. "Numerical Investigation of Ultrasonically Absorptive Coating for Hypersonic Laminar Flow Control," AIAA Paper 2017-2311, March 2017.

16. Wu, T., Cox, T. J., and Lam, Y. W. "From a Profiled Diffuser to an Optimized Absorber," *The Journal of the Acoustical Society of America*, Vol. 108, No.2, 2000, pp. 643-650.
doi: 10.1121/1.429596

17. Schwan, L., Geslain, A., Romero-García, V., and Groby, J. P. "Complex Dispersion Relation of Surface Acoustic Waves at a lossy Metasurface," *Applied Physics Letters*, Vol. 110, No. 5, 2017, 051902.
doi: 10.1063/1.4975120

18. Liu, T., Liang, S., Chen, F., and Zhu, J. "Inherent Losses Induced Absorptive Acoustic Rainbow Trapping with a Gradient Metasurface," *Journal of Applied Physics*, Vol. 123, No.9, 2018, 091702.
doi: 10.1063/1.4997631

19. Brès, G. A., Colonius, T., and Fedorov, A. V., "Acoustic Properties of Porous Coatings for Hypersonic Boundary-layer Control," *AIAA Journal*, Vol. 48, No. 2, 2010, pp. 267–274.
doi: 10.2514/1.40811

20. Brès, G. A., Colonius, T., and Fedorov, A. V., "Interaction of acoustic disturbances with micro-cavities for ultrasonic absorptive coatings," AIAA Paper 2008-3903, June 2008.

21. Bountin, D., Chimitov, T., Maslov, A., Novikov, A., Egorov, I., Fedorov, A., and Utyuzhnikov, S., "Stabilization of a Hypersonic Boundary Layer Using a Wavy Surface," *AIAA Journal*, Vol. 51, No.5, 2013, pp. 1203–1210.
doi: 10.2514/1.J052044

22. Zhao, R., Wen, C. Y., Tian, X. D., Long, T. H., and Yuan, W., "Numerical simulation of local wall heating and cooling effect on the stability of a hypersonic boundary layer," *International Journal of Heat and Mass Transfer* (to be published).

23. Egorov, I. V., Fedorov, A. V., and Soudakov, V. G., "Direct Numerical Simulation of Disturbances Generated by Periodic Suction-blowing in a Hypersonic Boundary Layer," *Theoretical and Computational Fluid Dynamics*, Vol. 20, No.1, 2006, pp. 41–54..

doi: 10.1007/s00162-005-0001-y